Chemical Geology 670 (2024) 122378

Contents lists available at ScienceDirect

Chemical Geology

journal homepage: www.elsevier.com/locate/chemgeo

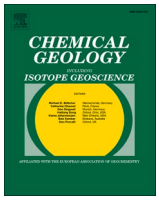

Seawater-oceanic crust interaction constrained by triple oxygen and hydrogen isotopes in rocks from the Saglek-Hebron complex, NE Canada: Implications for moderately low-$\delta^{18}O$ Eoarchean Ocean

A. Kutyrev [a,b,*], I.N. Bindeman [a], J. O'Neil [c], H. Rizo [d]

[a] University of Oregon, Eugene, United States of America
[b] School of Earth and Environmental Sciences Cardiff University, Cardiff, Wales, UK
[c] Dept. of Earth and Env. Sciences, University of Ottawa, Ottawa, Canada
[d] Dept. of Earth Sciences, Carleton University, Ottawa, Canada

ARTICLE INFO

Editor: Dr. S Aulbach

Keywords:
Triple oxygen isotopes
Water-rock interactions
Early Earth
Submarine hydrothermal systems
Oceanic crust

ABSTRACT

Estimations of Earth's earliest surface conditions assume a strong connection between the temperature and oxygen isotopic composition of oceans, balanced by surface weathering and submarine hydrothermal alteration. The oldest preserved supracrustal rocks provide rare opportunities to study and constrain the earliest surface conditions prevailing on the Earth. Here, we present a study of triple oxygen and hydrogen isotopes of hydrothermally altered Eoarchean metamorphosed basalts, ultramafic rocks, and detrital and chemical sediments, from the Saglek-Hebron Complex in northern Labrador, Canada. For the metavolcanic rocks, $\delta'^{18}O$ values range from 4.83 ‰ to 8.56 ‰, while $\Delta'^{17}O$ values vary from −0.076 ‰ to −0.023 ‰, both higher and lower than the mantle. Accounting for the effects of metamorphism on oxygen and hydrogen isotopic compositions, we demonstrate that triple oxygen isotopic values are preserved from the hydrothermal suboceanic stage, while none of the hydrogen isotope compositions (δD from −77.9 ‰ to −10.7 ‰) are interpreted as primary. Several metabasalt samples from the Saglek-Hebron Complex yielded $\Delta'^{17}O$ values lower than modern mantle values, which cannot be explained by direct interaction with modern seawater and indicate complex upstream interactions. Our numerical models and Monte Carlo simulation considers one- and two-stage mechanisms of water-rock interaction, including the $\delta'^{18}O$ and $\Delta'^{17}O$ isotopic shift effects due to interaction between basalts and chemical sediment-derived fluids. The modelling favors Eoarchean seawater characterized by low $\delta'^{18}O < -8$ ‰ at $\Delta'^{17}O$ up to 0.01 ‰. This model also works for higher $\Delta'^{17}O$ at lower $\delta'^{18}O$. Our results also suggest that without proper modelling of multi-stage water-rock interaction, involving isotopic shifts and input of sediment-derived fluids, exposed sections of altered oceanic crust present only remote evidence of the original seawater. Due to the modeled isotopic shifts and fluid mixing, we favor "weak" coupling of seawater-oceanic crust interaction globally. This potentially reduces the relative importance of submarine hydrothermal alteration in explaining the oxygen isotopic record in submarine basalts across the geologic history.

1. Introduction

Estimations of Earth's surface temperatures during approximately the first half of its history range from intensely hot to mild conditions, akin to today's climate. Constraining the surface conditions prevailing on the early Earth is crucial for our understanding of major geological events such as the start of plate tectonics, continent formation, 'Snowball Earth' events, atmospheric oxygenation, and biological diversification (Lyons et al., 2014; Dodd et al., 2017; Bauer et al., 2020; Lepot, 2020). Characterizing Earth's earliest hydrosphere, including its volume, temperature, as well as chemical and isotopic composition, relies on investigations of ancient rocks whose protoliths preserved their original isotope compositions, despite post-emplacement processes such as metamorphism or metasomatism. The gradual temporal increase in $\delta^{18}O$ observed in cherts and carbonates throughout Earth's history is a longstanding enigma in geosciences that has been debated for over 50 years (Perry, 1967; Jackson and Shaw, 1975; Muehlenbachs and Clayton, 1976; Knauth and Lowe, 2003; Johnson and Wing, 2020; Liljestrand

* Corresponding author at: School of Earth and Environmental Sciences, Cardiff University, Main Building, Park Place, Cardiff CF10 3AT, UK.
E-mail address: KutyrevA@cardiff.ac.uk (A. Kutyrev).

https://doi.org/10.1016/j.chemgeo.2024.122378
Received 6 March 2024; Received in revised form 7 August 2024; Accepted 31 August 2024
Available online 1 September 2024

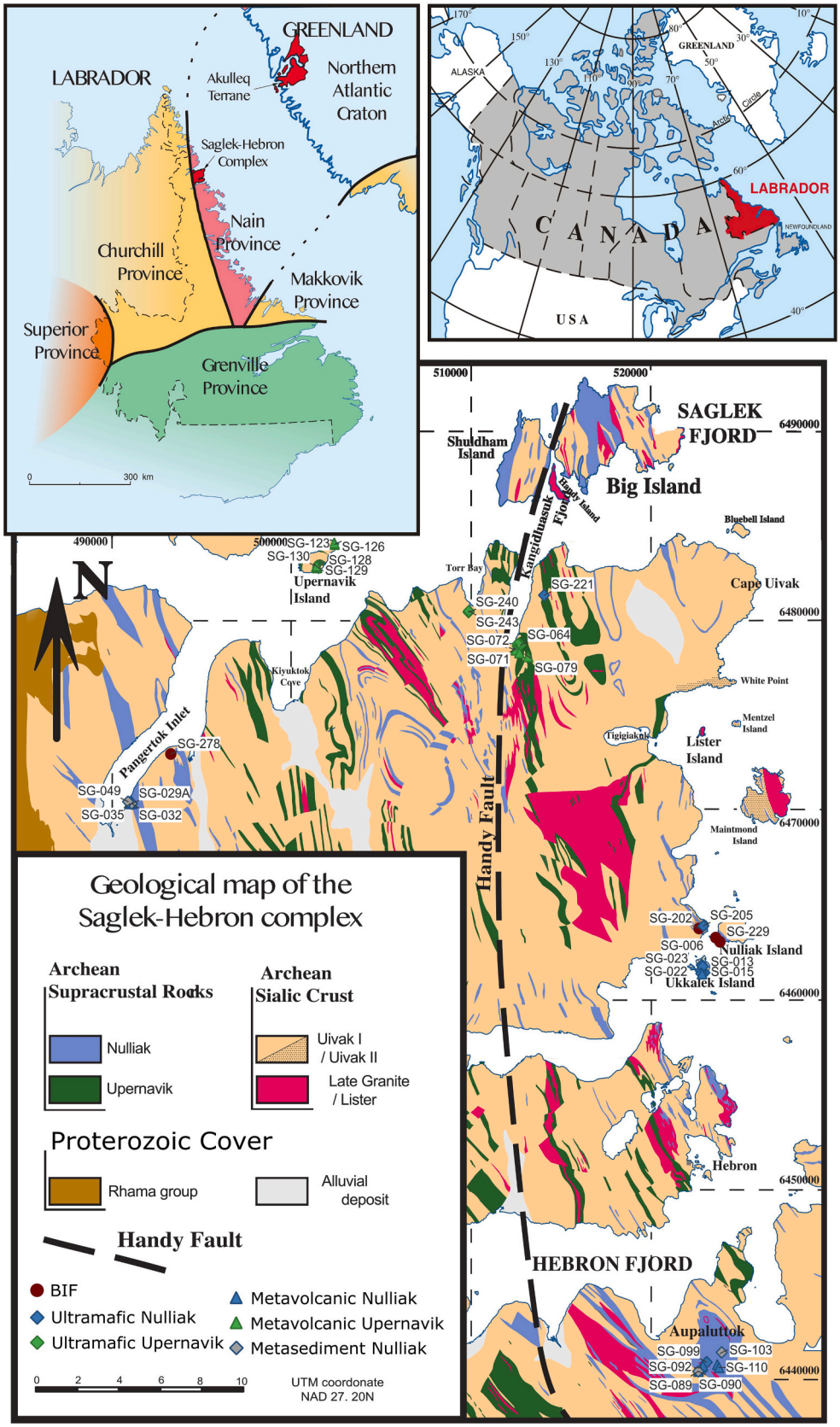

Fig. 1. Geological map of the Saglek-Hebron Complex, modified from (Ryan and Martineau, 2012; Komiya et al., 2015; Wasilewski et al., 2019; Wasilewski et al., 2021). Detailed GPS locations for each sample can be found in Table S1. The Nulliak and Upernavik Archean supracrustal rocks include mafic metavolcanic rocks, ultramafic and metasedimentary rocks. Coordinates are in UTM NAD 27 zone 20. (For interpretation of the references to colour in this figure legend, the reader is referred to the web version of this article.)

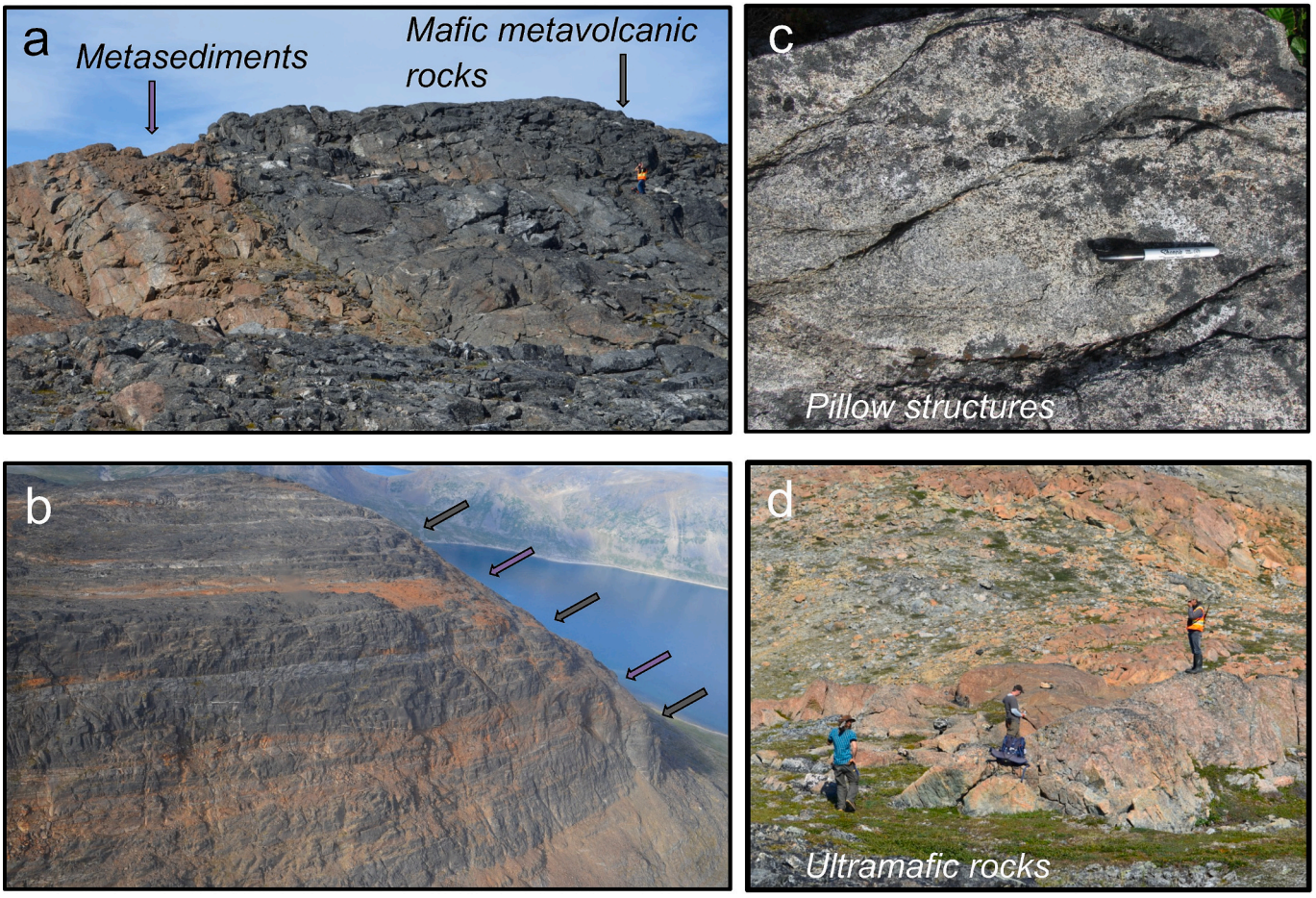

Fig. 2. Field photographs of the Saglek-Hebron Complex formations. a) and b) Contacts and interbedding between quartz-biotite-garnet metasedimentary rocks (shown with purple arrows) and mafic metavolcanic rocks (shown with grey arrows), c) pillow structures in metabasalts, d) outcrops of metamorphosed ultramafic rocks. (For interpretation of the references to colour in this figure legend, the reader is referred to the web version of this article.)

et al., 2020; Bindeman, 2021). Two competing explanations have been proposed to account for the temporal increase in $\delta^{18}O$ observed in sedimentary proxies. The first suggests a change in seawater $\delta^{18}O$ over time. In chemical sedimentary rocks, because $\delta^{18}O_{rock}$ depends on both, the $\delta^{18}O_{seawater}$ and temperature, a scenario involving a secular change of $\delta^{18}O_{seawater}$ implies that the temperature of the surface environment has remained relatively constant (and hospitable for life), comparable to modern conditions (ca. 0 to +29 °C in non-polar regions) (Veizer et al., 1999; Kasting et al., 2006; Jaffrés et al., 2007; Galili et al., 2019; Isson and Rauzi, 2024). However, the geologic record of panglobal Snowball Earth glaciations and less extensive continental glaciations suggest unsteady global temperature through time, which could plunge for tens of millions of years. Moreover, moderate and occasionally cold climate attests that $\delta'^{18}O$ of seawater must have increased by ~15 ‰ since the Archean to account for constant $\Delta'^{17}O\ (T)_{rock\text{-}water}$ values.

The second hypothesis proposed to explain the temporal increase in $\delta^{18}O$ states that the isotopic composition of seawater remained constant ($\delta^{18}O_{seawater} = 0 \pm 2$ ‰) over time (Knauth and Lowe, 2003; Robert and Chaussidon, 2006), primarily based on crust-mantle-hydrosphere global box models (Muehlenbachs and Clayton, 1976; Holland, 1984). Because of the dependence between $\delta^{18}O$ of a sedimentary rock and water temperature, this model requires that the early ocean was much hotter than it currently is, from 70 °C to as high as 110 °C (Chase and Perry, 1972; McGunnigle et al., 2022), where greater pH_2O atmospheric pressures would account for seemingly unrealistic higher than boiling temperatures (Chase and Perry, 1972). These mechanisms involve balance of high- and low-temperature interactions between seawater and the oceanic crust, resulting in the enrichment and depletion of ^{18}O in seawater, respectively. Estimated high-temperature hydrothermal alteration fluxes at mid-ocean ridges is the dominant mass flux (80–90 %) into the hydrosphere, followed by surface weathering (10–20 %) (Wallmann, 2001) and less important fluxes such as recycling of water or continental growth. However, the uncertainty in estimating the magnitude of these fluxes exceeds an order of magnitude (Gregory and Taylor, 1981; Holland, 1984; Muehlenbachs, 1998), and the hydrosphere would respond to changes on a 10^7–10^8 year-scale (Holland, 1984).

One of the reasons for the existence of contrasting models is that an equation describing oxygen isotope fractionation during water/rock interaction is dependent on both temperature and $\delta^{18}O_{water}$. The addition of ^{17}O isotopic data, however, provides an independent equation within the same isotopic system, potentially making the whole system solvable for both isotopic composition and temperature. This new approach applied to previously well-studied outcrops provides fresh insights into the water/rock interaction processes. We here present a comprehensive triple O and D/H study of ~3.8 Ga to ~3.4 Ga rocks from the Saglek-Hebron Complex (northern Labrador, NE Canada), a rare remnant of Eoarchean oceanic crust. Samples studied include metamorphosed basaltic, ultramafic and sedimentary rocks (cherts and banded iron formations (BIF)). Mathematical and Monte Carlo simulations allow to model the effects of water-rock interaction and to derive $\delta'^{18}O$ and $\Delta'^{17}O$ values of parental waters at variable water-rock ratios and mixing, that can be applied in similar studies.

Table 1
Isotopic compositions of different lithologies studied.

Lithology	n	δ'^{18}O mean	δ'^{18}O min	δ'^{18}O max	Δ'^{17}O mean	Δ'^{17}O min	Δ'^{17}O max	δD mean	δD min	δD max
BIF	1	8.24	7.69	8.78	−0.051	−0.051	−0.051	−45.67	−45.67	−45.67
Ultramafic Nulliak	7	5.24	2.49	8.08	−0.052	−0.095	−0.026	−46.25	−52.52	−38.91
Ultramafic Upernavik	1	5.97	5.09	6.86	−0.034	−0.034	−0.034	−45.79	−55.46	−38.88
Mafic metavolcanic Nulliak	8	6.43	4.83	8.56	−0.051	−0.073	−0.030	−41.91	−55.06	−10.71
Mafic metavolcanic Upernavik	9	6.62	4.92	7.55	−0.049	−0.076	−0.023	−34.89	−63.45	−15.71
Metasediment Nulliak	2	6.38	6.04	6.61	−0.027	−0.031	−0.023	−55.15	−74.18	−42.23

Full data is available in Supplementary Table S1.

2. Geological setting

The Saglek-Hebron Complex (SHC) is located in northern Labrador, Canada, within the Archean Nain Province of the North Atlantic Craton (Fig. 1). It is a granite-greenstone terrane mostly composed of orthogneisses from the tonalite-trondhjemite-granodiorite (TTG) series and including sub-km to km scale enclaves of supracrustal assemblages. The SHC has been metamorphosed to granulite facies to the west of the Handy fault, and amphibolite facies to the east, with the southeastern area believed to have reached granulite conditions and retrogressed to amphibolite facies (Bridgewater et al., 1975; Schiøtte et al., 1986).

The SHC felsic rocks were formed through multiple magmatic events from approximately 3.9 Ga to 2.7 Ga (Komiya et al., 2015; Shimojo et al., 2016; Wasilewski et al., 2021). The oldest felsic component consists of banded grey gneiss referred to as the Iqaluk gneiss (sometimes called the Nanok gneiss). It has been dated at 3920 ± 49 Ma (Shimojo et al., 2016), but this age was questioned (Whitehouse et al., 2019) and a slightly younger age of 3869 ± 6 Ma was subsequently obtained for the same rocks (Wasilewski et al., 2021). Other felsic units include the ca. 3750 Ma Uivak I gneiss, the ca. 3600 Ma Uivak II gneiss, the ca. 3330 Ma Iluilik gneiss, the ca. 3230 Ma Lister gneiss, and 2700–2800 Ma granitic rocks (e.g., Wasilewski et al., 2021).

The supracrustal rocks of the SHC mostly consist of mafic amphibolites interpreted as basaltic metavolcanic rocks (Nutman et al., 1989), locally preserving pillow lava structures (Fig. 2; Wasilewski et al., 2019). These mafic metavolcanic rocks exhibit tholeiitic-like geochemical affinities, with compositional variation consistent with fractional crystallization within volcanic flows (Wasilewski et al., 2019). The supracrustal rocks have been divided into two distinct assemblages based on the presence or absence of crosscutting Paleoarchean dykes called the Saglek dykes (Baadsgaard et al., 1979). The Nulliak supracrustal unit intruded by the Saglek dykes, is interpreted to be older than the rocks from the Upernavik assemblage, which does not appear to be intruded by the Saglek dykes. Ages for the mafic metavolcanic rocks are not as well constrained as for the felsic gneisses dated by U—Pb on zircon, but Sm—Nd and Lu—Hf isochron ages suggest an Eoarchean age of nearly 3.8 Ga for the Nulliak assemblage, and a Paleoarchean age of ~3.4 Ga for the Upernavik unit (Morino et al., 2017; Morino et al., 2018). Metavolcanic rocks from both supracrustal assemblages are interlayered with quartz-biotite-garnet schists interpreted as detrital metasedimentary rocks (Collerson et al., 1991). Chemical metasediments such as BIF and chert-like quartzites can be found within the Nulliak assemblage (e.g., Bridgewater et al., 1975; Baadsgaard et al., 1979), but appear to be absent in the Upernavik volcano-sedimentary unit (Bridgewater and Schiøtte, 1977).

The SHC comprises ultramafic rocks that can be spatially associated with the supracrustal units, but more commonly occurring as large ultramafic bodies within the felsic gneisses. These ultramafic rocks have been described as metakomatiites and fragments of lithospheric mantle (Collerson et al., 1991), but Wasilewski et al. (2019) rather interpreted them as olivine-rich cumulates derived from parental magmas with komatiitic basalt compositions. The ultramafic rocks include 2 distinct groups that have different Fe contents, Al/Ti ratios and trace element compositions. The low-Fe ultramafic rocks seem to be related to the Nulliak mafic metavolcanic rocks through magmatic differentiation, whereas the high-Fe ultramafic rocks appear geochemically unrelated to the basaltic rocks from either the Nulliak or the Upernavik assemblages (Wasilewski et al., 2019).

3. Samples and Methods

3.1. Samples

We report triple O ($\delta^{18}O$, $n = 40$; $\Delta^{17}O$, $n = 28$) and H (δD, $n = 44$) isotopic compositions on several rock types from the SHC, including samples of mafic metavolcanic rocks, ultramafic rocks and metasedimentary rocks (detrital and BIF). The isotopic data obtained on these samples is presented in Table 1 and Supplementary Table S1 (this table also features whole-rock geochemical data previously published in (Wasilewski et al., 2019).

3.2. Analytical methods

All stable isotope analyses were performed at the Stable Isotope Lab of the University Oregon (USA) using a Thermo Scientific MAT253 mass spectrometer. We report data using three preparation methods: $\delta^{18}O$ by laser fluorination as CO_2 gas, $\delta^{18}O$ and $\Delta'^{17}O$ values as O_2 gas, and δD + H_2O runs by thermal conversion elemental analyzer (TCEA). Oxygen isotope analyses were conducted either using a regular plug (holding multiple samples) or an airlock sample chamber. Analyses conducted using the latter were performed for reactive samples. San Carlos Olivine ($\delta^{18}O = 5.24$ ‰, $\Delta'^{17}O = -0.052$ ‰), UWG2 garnet ($\delta^{18}O = 5.80$ ‰) (Valley et al., 1995) and an in-house UOG garnet standard ($\delta^{18}O = 6.52$ ‰) were used to calibrate the data on the VSMOW scale. Measurement precision was ±0.1 ‰ for $\delta^{18}O$, ±0.01 ‰ for $\Delta'^{17}O$, ±0.02–0.04 wt% for the H_2O content, and within 1–3 ‰ for δD. Note that we use $\Delta'^{17}O_{mantle} = -0.052$ ‰ ($\theta = 0.528$) from Sharp and Wostbrock (2021). To check the dependence of our modelling we conduct two-stage simulation (described in discussion) using $\Delta'^{17}O_{mantle} = -0.052$ ‰ ($\theta = 0.5305$) or − 0.037 if $\theta = 0.528$ from Miller et al. (2020) (Supplementary Fig. S1). The small difference observed is not crucial for the goals of this paper.

3.3. Isotopic notations and fractionation equations

In addition to conventionally defined $\delta^{18}O$ and $\delta^{17}O$ values as $(R_{sample}/R_{VSMOW} - 1)\cdot 1000$ where R is $^{18}O/^{16}O$ and $^{17}O/^{16}O$ ratios in samples and VSMOW is water standard (Sharp et al., 2016), we used primed notations of $\delta'^{18}O$ and $\delta'^{17}O$. Primed, or linearized δ values are expressed as in (Miller and Pack, 2021), where:

$$\delta'^{18,17}O = 1000ln\left(\delta^{18,17}O/1000 + 1\right) \quad (1)$$

There are no numerically significant differences from conventionally defined δ's (typically by 0.0×‰), but the transformation using the logarithmic scale allows for simple algebra when relating isotope fractionations $1000\ln\alpha^{18}O$ and $\delta'^{18}O$ values. In primed coordinates:

$$\Delta'^{18}O_{proxy-water}(T) = \delta'^{18}O_{proxy}(T) - \delta'^{18}O_{water}(T) \quad (2)$$

A similar equation holds for ^{17}O. Eq. (2) relates measured and

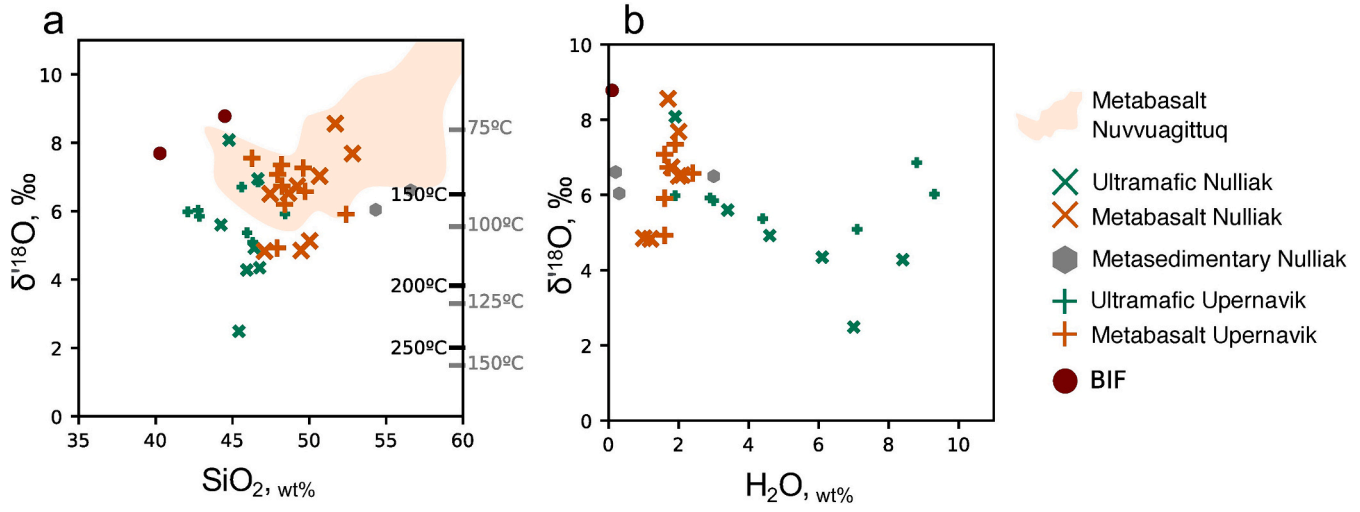

Fig. 3. a) $\delta^{18}O$ vs. SiO_2 diagram for the Saglek-Hebron Complex rocks. Tick marks show equilibrium temperatures using basalt-water fractionation using with the modern 0 ‰ SMOW seawater (black) and assumed Archean seawater ($\delta^{18}O = -5$ ‰, grey) for basalt at various temperatures, b) Correlation between $\delta^{18}O$ and water content; note the high water content in some ultramafic rocks reflecting serpentinization. The orange field shows the Nuvvuagittuq 4.3–3.8 Ga metabasalts (Bindeman and O'Neil, 2022).

linearized $\delta'^{18}O$ and $\delta'^{17}O$ values with temperature-dependent fractionation factors is strictly as:

$$1000ln\alpha^{18}O_{proxy-water}(T) = \Delta'^{18}O_{proxy-water}(T) \quad (3)$$

The linearized notations allow the $\Delta'^{17}O$ to be expressed as:

$$\Delta'^{17}O = \delta'^{17}O - 0.528 \cdot \delta'^{18}O \quad (4)$$

In a linearized format, the equilibrium fractionation of $^{17}O/^{16}O$ relative to $^{18}O/^{16}O$ between two phases x and y is given by the equation:

$$\delta'^{17}O_x - \delta'^{17}O_y = \theta \cdot (\delta'^{18}O_x - \delta'^{18}O_y) \quad (5)$$

The θ value varies with temperature ranging from 0.5305 at $T \rightarrow \infty$ to lower values at $T = 273.15$ K. To by first order of approximation, the temperature dependence of θ for quartz is given by Sharp et al. (2016):

$$\theta_{x-y} = -\frac{1.85}{T} + 0.5305 \quad (6)$$

3.4. Fractionation factors

We calculated the fractionation factors for basalt/water interaction, on the basis of average normative (CIPW) composition based on XRF analysis for the studied metavolcanic rocks. The original mineral assemblage in the basaltic rocks could have been different, perhaps including glass. However, given that fractionation factors are mainly dependent on SiO_2, FeO and, to a lesser extent, Al_2O_3 contents, this approach is likely robust, and allows for calculating reasonable

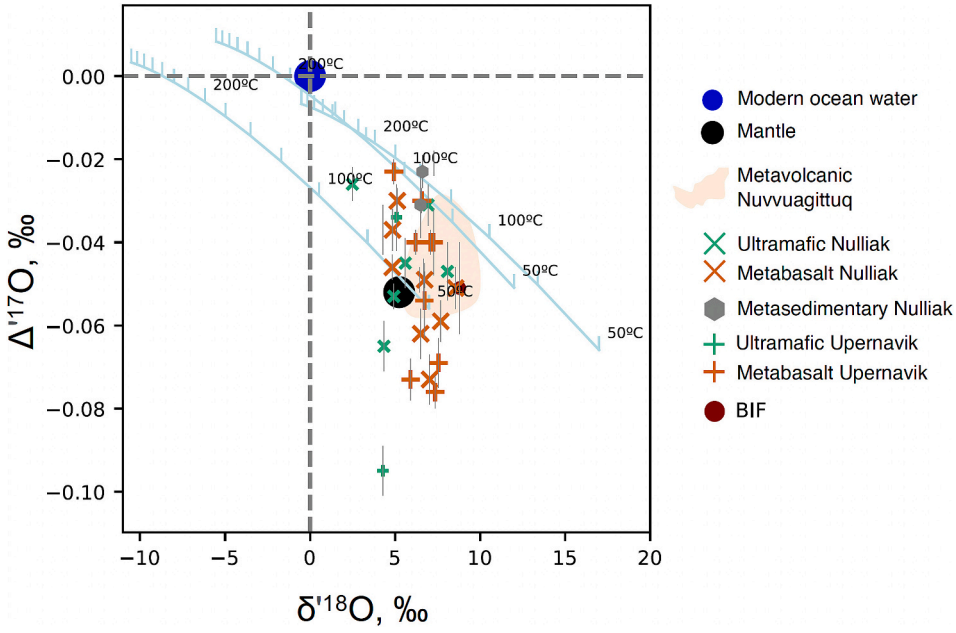

Fig. 4. Triple oxygen isotope data for the studied rocks from Saglek-Hebron Complex, compared to the mantle and $\Delta'^{17}O$-$\delta'^{18}O$ fractionation curves. Each of three curves corresponds to a different starting seawater composition (Archean-I, $\delta'^{18}O = -10$ ‰, $\Delta'^{17}O = 0.01$ ‰, Archean-II, $\delta'^{18}O = -5$ ‰, $\Delta'^{17}O = 0.015$ ‰, and modern, $\delta'^{18}O = 0$ ‰, $\Delta'^{17}O = 0$ ‰). Note overlap between 3.8 and 3.4 Ga metavolcanic ultramafic rocks, as well as between them and 4.3–3.8 Ga Nuvvuagittuq metabasalts (Bindeman and O'Neil, 2022), marked by the orange field.

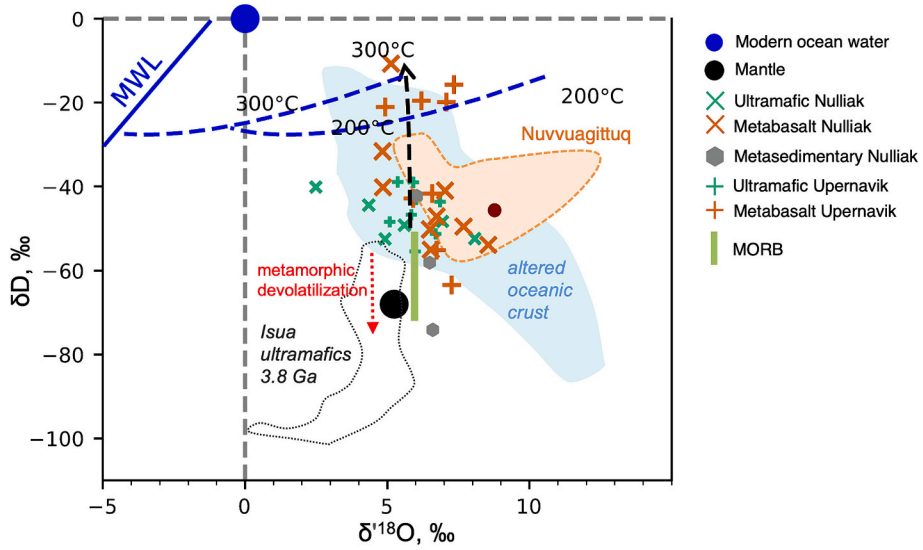

Fig. 5. Hydrogen and oxygen isotope data for studied samples of Saglek-Hebron Complex. Mid-ocean ridge basalts values after Dixon et al. (2017); modern altered oceanic crust after Bowers and Taylor (2012), Alt and Teagle (2003), Stakes and O'Neil (1982); Isua after Pope et al. (2012). Note almost complete overlap between 3.8 Ga Nulliak volcanics and modern altered oceanic crust. Also, note that 3.8 Ga Nulliak ultramafic rocks are significantly less depleted then 3.8 Ga Isua ultramafic rocks. The orange field marks Nuvvuagittuq 4.3–3.8 Ga metabasalts (Bindeman and O'Neil, 2022). Equilibrium Isotopic fractionations with modern seawater are shown by dashed blue lines; red subvertical line shows the effect of metamorphic devolatilization calculated for an altered basalt with 10 wt% start 0.9 wt% final H_2O content; vertical black line shows the effect of seawater addition (addition of meteoric water with $\delta D > -20$ ‰ with have roughly the same effect). (For interpretation of the references to colour in this figure legend, the reader is referred to the web version of this article.)

fractionation factors. The fractionation factors for each mineral (for both $\delta'^{18}O$ and $\Delta'^{17}O$) were taken from Schauble and Young (2021). Because this database provides fractionation factors for Fe-free minerals, all iron was recalculated as hematite; the relevant fractionation factors were taken from Hayles et al. (2018). For altered basalt we assumed a 50:50 mix of primary and secondary minerals, namely half of the primary orthopyroxene and diopside were hydrothermally altered to serpentine and tremolite, respectively, and 100 % of primary albite was converted to kaolinite. Subsequently, we derived polynomial fits for both parameters for altered basalt-water fractionation:

$$\delta'^{18}O_{basalt-water} = 10^6 \cdot 3.75/T^2 - 10^3 \cdot 6.12/T \quad (7)$$

$$\Delta'^{17}O_{basalt-water} = -3,409,768/T^3 + 1119.55/T^2 + 13.77/T - 0.0181 \quad (8)$$

The computed differences between integral fractionations factor for altered and primary basalt with water are determined to be negligible at $T > 50$ °C. The details of the calculations of the fractionation factors for each mineral and basalt are presented in the Supplementary Materials spreadsheet "Fractionation factors". Fractionation equations for $\delta'^{18}O$ from Vho et al. (2019) are shown for comparison, as they were obtained by the different methods. The equations above are compared with fractionation equations from Bindeman and O'Neil (2022). The difference in $\delta'^{18}O$ ranges from 0.66 ‰ at low temperature, to 2 ‰ at high temperature, and from 0.007 ‰ to 0.015 ‰ for $\Delta'^{17}O$, respectively. This difference is explained by different basalt compositions used by Bindeman and O'Neil (2022) and by small discrepancies between theoretically calculated and experimentally determined fractionation curves.

4. Results

4.1. Oxygen isotopes and temperature of water-rock interaction

Table 1 presents the stable isotope data summarized as averages for each lithology. The full isotopic dataset for individual samples is found in the Supplementary Table S1. In general, the SHC metavolcanic rocks $\delta^{18}O$ values of 5–8.5 ‰ are within the range of modern oceanic floor basalts affected by low- and moderate temperatures hydrothermal alteration (<200 °C, Figs. 3, 4), and no low-$\delta^{18}O$ values indicating high-T interaction have been recorded.

Comparing metavolcanic rocks from the Eoarchean Nulliak and Paleoarchean Upernavik units, no significant difference in $\delta^{18}O$ values is observed; with mean values of 6.43 ± 1.23 ‰ and 6.62 ± 0.84 ‰ respectively, both higher than the typical mantle-derived basalt at 5.7 ± 0.2 ‰ (Eiler, 2001). Similarly, no significant difference is evident between ultramafic rocks from the different units, as the samples interpreted to be associated with the Nulliak assemblage yielded a mean $\delta^{18}O$ value of 5.24 ± 1.85 ‰, while the mean $\delta^{18}O$ value for the samples related to the Upernavik assemblage is 5.97 ± 0.60 ‰. The detrital metasediments, have similar or identical composition, while banded iron formation (BIF) tends to display $\delta^{18}O$ values toward the upper range, with a mean $\delta^{18}O$ value of 8.24 ± 0.77 ‰.

The measured $\delta^{18}O$ values of mafic metavolcanic rocks correspond to a rock-water interaction temperature range of 125–180 °C (Fig. 3a) if modern seawater (i.e. $\delta^{18}O = 0$ ‰) is taken as the reacting fluid. The $\delta^{18}O$ values of the SHC mafic-ultramafic rocks partly overlap with the 4.3–3.8 Ga metabasalts from the Nuvvuagittuq Greenstone Belt, NE Canada. (Bindeman and O'Neil, 2022).

4.2. Triple oxygen isotopes

The majority of SHC samples exhibit triple oxygen isotope compositions around mantle values, extending to slightly higher and lower $\Delta'^{17}O$ values (Fig. 4). Composition of samples from both Nulliak and Upernavik assemblages are in the same range, with a number of metavolcanic rock samples unexpectedly showing $\Delta'^{17}O$ values lower than the mantle composition (−0.052 ‰). The compositional range of the ultramafic rocks completely overlaps with the metavolcanic rocks, with the exception of one ultramafic sample showing a more depleted composition ($\Delta'^{17}O = -0.095$ ‰). The SHC metasedimentary rocks lie on the modern SMOW fractionation line with the BIF exhibiting lower $\Delta'^{17}O$ values. Although showing a larger extent of variation, the triple oxygen isotope compositions of the SHC rocks are mostly comparable to the Nuvvuagittuq metavolcanic rocks (Fig. 4).

4.3. Hydrogen isotopes

No significant difference has been observed for hydrogen isotope compositions between whole-rock samples and hornblende separates (Table 1 and Supplementary Table S1). The majority of the SHC rocks show δD values between −30 and − 60 ‰ (Fig. 5), except for a group of 5 metavolcanic samples with higher δD values ranging from −10 to −21 ‰, four of which were collected on the Upernavik Island in close proximity to one another (Fig. 1).

5. Discussion

5.1. Potential influence of metamorphism on triple O isotope compositions

The mafic metavolcanic rocks of the SHC represent rare remnants of early oceanic crust that potentially provide insight into the coeval hydrosphere via their stable isotopic compositions. However, as rocks from the SHC have been metamorphosed to at least upper-amphibolite and up to granulite facies in some areas, we first need to evaluate their potential to preserve the pre-metamorphism O isotopic values and discuss the effects that metamorphism could have had on their original compositions. The SHC is currently located at high latitudes, hence not affected by lateritic weathering, or, if such weathering occurred in previous times, its products were removed by glacial scouring. Therefore, we do not consider that recent weathering affected the O isotopic composition of the analyzed samples. We also discount the effects of secondary (post-metamorphic) exchange with meteoric or hydrothermal fluids, as there is limited evidence for post-metamorphic alteration in the studied samples and weathered surface and fractures were carefully removed during sample preparation.

Although limited, data on metamorphic rocks from previous studies also suggest that primary pre-metamorphism triple O isotope compositions are largely preserved, as was earlier argued for the 4.3–3.8 Ga Nuvvuagittuq rocks (Bindeman et al., 2022). Peters et al. (2020) demonstrated that olivine and orthopyroxene from Archean rocks serpentinized by 2.7 Ga seawater, and subsequently de-serpentinized at ~1.8 Ga, preserved their original low-$\delta'^{18}O$ and high-$\Delta'^{17}O$, recording the interaction with the seawater and temperature at which it occurred. Previous work on hydrothermally altered rocks from the Karelia Archean block (East Baltic Shield), later metamorphosed to amphibolite facies, also demonstrated preservation of the world's lowest $\delta'^{18}O$ (−27.5 ‰) protolithic values (Bindeman and Serebryakov, 2011). We, therefore, consider the O isotope compositions measured in the SHC rocks to largely reflect their hydrothermal history prior to the regional amphibolite-granulite facies metamorphic event.

In order to assess how water loss affects $\delta'^{18}O$ and $\Delta'^{17}O$ values during metamorphic dehydration reactions, we have performed Rayleigh fractionation models. To do so, we used the average basalt composition, estimated the possible assemblage of secondary minerals produced by its alteration (variable amounts of chlorite, epidote, and serpentine together with residual plagioclase and clinopyroxene) and calculated $\delta'^{17}O$ and $\delta'^{18}O$ values of the altered rock (Supplementary Material "Oxygen_metam_dehydration"; Fig. S2). Subsequently, we calculated gradual dehydration along several metamorphic P-T paths resulting in successive metamorphic assemblages (Schmidt and Poli, 1998). Our modelling shows no significant shift in both $\delta'^{18}O$ and $\Delta'^{17}O$ regardless of the input conditions (water/rock ratio and proportions of primary and secondary minerals in the alteration products) or metamorphic P-T paths. Therefore, it is possible to shift $\delta^{18}O$ and $\Delta'^{17}O$ by equilibration with relevant water and preserve the acquired composition during almost complete metamorphic dehydration.

Hydrogen isotopic compositions for the SHC rocks display a different behavior during metamorphism, as the D/H ratio is strongly controlled by the total balance of H_2O, and to a lesser extent by the dehydration/rehydration history. Isotopic partitioning during metamorphism fractionates compositions toward heavier δD (due to departing H_2O and remaining OH). Therefore, the effects of metamorphic devolatilization would have shifted δD compositions to approximately 50 ‰ lower values (Fig. 5) relative to starting composition of the rocks hydrothermally altered by present-day seawater. However, despite inferred metamorphic transformation, the δD values of the SHC samples overlap with those of modern altered oceanic crust (Fig. 5). Similar to the Nuvvuagittuq metavolcanic rocks, the SHC metavolcanic rocks have δD values slightly higher than expected, given their high metamorphic grade, which may imply that the δD of the Eoarchean oceanic crust was higher. These two examples of early oceanic crust, however, contrast with the low δD characterizing the Eoarchean ultramafic rocks from the Isua supracrustal belt (SW Greenland, Pope et al., 2012), whose composition can be explained by the metamorphic devolatilization (dotted red line on Fig. 5) of the oceanic crust altered by seawater with modern-day δD. We, however, also consider the potential for addition of isotopically heavier water though rehydration, for example from deeper devolatizing portions of the oceanic crust. This would affect δD but have a negligible effect on oxygen isotope compositions, in agreement with the observed data (black dashed arrow on Fig. 5). The same process can explain the high-δD samples from Upernavik island, if a greater volume of added water is assumed.

Thus, as the δD of the SHC rocks is inconsistent with fluxing of exotic fluids through the rocks since their formation (Fig. 5), it also implies that O isotopes were not affected by such process.

5.2. Implications of the isotopic variations

Measured $\delta'^{18}O$ of the SHC metavolcanic rocks is suggestive of alteration at temperatures between 125 and 180 °C, assuming that the composition of Eoarchean seawater was identical to that of modern ocean (Fig. 3). This is within a reasonable temperature range but slightly warmer than the typical temperatures for seafloor basalt alteration (<150 °C, Alt and Teagle, 2003'Zhang, 2014 #8067). When assuming a composition of $\delta'^{18}O$ of −5 ‰ for the Archean seawater, the temperature range for the SHC metabasalts decreases to 75–120 °C (Grossman and Joachimski, 2022). No correlation between $\delta'^{18}O$ and silica content is observed (Fig. 3a), which indicates that possible later silicification did not impact the oxygen isotopic compositions of the volcanic rocks (Bindeman and O'Neil, 2022). Similarly, no clear relationship was found between water content and $\delta'^{18}O$ for the metavolcanic rocks (Fig. 3b). Ultramafic rocks exhibit a high variability in water content, but still show no correlations with $\delta'^{18}O$ (Fig. 3b).

In $\Delta'^{17}O$–$\delta'^{18}O$ space (Fig. 4), the majority of the SHC metavolcanic rocks yield low-$\Delta'^{17}O$ that cannot be interpreted as a result of equilibrium fractionation between rock and modern seawater with $\delta'^{18}O \approx 0$ ‰ (SMOW). Much more ^{18}O-depleted water, matching hypothetical Archean seawater estimates (i.e., −5 or − 10 ‰) is required. This seems to provide solid evidence for isotopically light Eoarchean oceans. It is also noteworthy that some of the 4.3–3.8 Ga Nuvvuagittuq samples similarly plot close to the fractionation line between −10 ‰ water and mantle (Fig. 4). However, the large span of the SHC $\Delta'^{17}O$ values, intercepting several fractionation lines, suggests the involvement of more complex processes than equilibrium fractionation, at least for some SHC samples studied here.

5.3. Potential sources of low- $\Delta'^{17}O$ water

There are several ways of producing low-$\Delta'^{17}O$ rocks, including alteration by low-$\delta'^{18}O$ oceanic waters, alteration by meteoric waters, addition of exotic low-$\Delta'^{17}O$ waters (i.e., those produced by evaporation), or participation of low-$\Delta'^{17}O$ dissolved atmospheric oxygen produced by mass-independent fractionation during atmospheric ozone production. In this section, we examine how these scenarios could apply the studied Archean rocks.

1. Alteration by meteoric waters that might have $\delta'^{18}O$ and $\Delta'^{17}O$ values of −10 ‰ and 0.03 ‰ respectively (Luz and Barkan, 2010) could

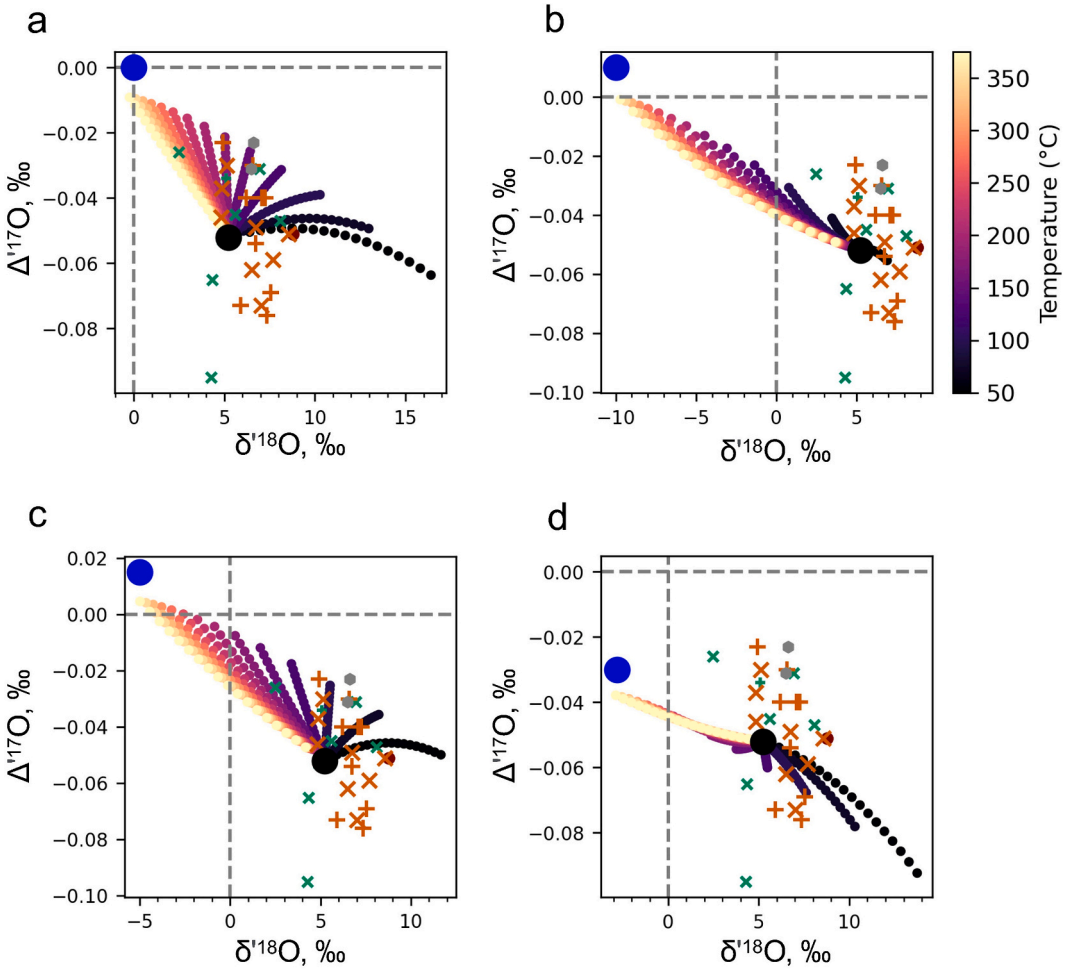

Fig. 6. One-stage modelling of potential effects of water-rock interaction on triple oxygen isotopic rock compositions resulting from interaction with modern seawater (a), Archean seawaters with assumed $\delta'^{18}O = -10$ ‰, $\Delta'^{17}O = 0.01$ ‰ (b) and $\delta'^{18}O = -5$ ‰, $\Delta'^{17}O = 0.015$ ‰ (c), and evaporitic water $\delta'^{18}O = -2.8$ ‰, $\Delta'^{17}O = -0.03$ ‰ (d). Samples are plotted as in Fig. 5. Python code and instructions are available in the Supplementary Materials.

satisfy low $\Delta'^{17}O$ data points. This scenario is unlikely because the submarine origin of the SHC basalts is well supported by pillow-lava structures and occurrence of BIF within some of the supracrustal assemblages (Wasilewski et al., 2019).

2. Evaporation of meteoric waters may lead to a range of waters enriched in ^{18}O and depleted in ^{17}O, for example, waters characterized by $\delta'^{18}O = +2.5$ ‰ and $\Delta'^{17}O$ of approximately -0.03 ‰ (Surma et al., 2021). Two issues, however, make this scenario unlikely. First, it is not clear if/how much dry land, a prerequisite for evaporite formation, existed in the early Archean (Korenaga, 2021). Second, a setting where evaporation of meteoric waters would occur also is inconsistent with a submarine origin for the SHC metavolcanic rocks, as described above.

3. Interaction with pre-existing evaporites, whose sulfates inherit extremely low $\Delta'^{17}O$ from atmospheric oxygen, was suggested by Peters et al. (2019) as the cause of the low $\Delta'^{17}O$ of Phanerozoic magnetite ores. However, this mechanism is not suitable for Eoarchean rocks because the formation of extremely low-$\Delta'^{17}O$ requires the presence of sufficient ozone (very high-$\Delta'^{17}O$) in the upper layers of the atmosphere, that lowers the $\Delta'^{17}O$ values of the remaining O_2 to as low as -0.5 ‰. As O_2 concentration in the air was likely low, evaporitic mechanisms are unlikely to occur before the 2.4 Ga Great Oxidation Event.

Since no known mechanisms are responsible for the isotopic compositions observed in the SHC rocks, we consider previously unexplored details of water-rock interaction, that includes a combination of isotope fractionation between seawater and rock, and mixing of fluids. Such processes have been previously proposed to explain $\delta^{18}O$ compositions of hydrothermally altered rocks and so-called "shifted" waters (Taylor Jr., 1971). We here pursue this early study forward by considering the effects on both $\delta'^{18}O$ and $\Delta'^{17}O$ values.

5.4. *Modelling $\delta'^{18}O$ and $\Delta'^{17}O$ in oceanic rocks*

In order to model $\delta'^{18}O$ and $\Delta'^{17}O$ in oceanic rocks interacting with seawater with different starting $\delta'^{18}O$ and $\Delta'^{17}O$ values, we used both fractionation (Hayles et al., 2018; Schauble and Young, 2021) and mixing equations (Wostbrock and Sharp, 2021) in triple oxygen space (the Python code and instructions are provided in Supplementary Material and in online repository: Kutyrev et al. (2024)). We considered one-stage and two-stage models of water-rock interaction and fluid mixing, as well as Monte Carlo simulation of $\delta^{18}O$ and $\Delta'^{17}O$ values in rocks and waters. Given our dataset, we selected a starting composition of seawaters and subsequent shifted waters resulting from water-rock interaction to explain the range of $\delta'^{18}O$ and $\Delta'^{17}O$ observed in the rock samples and their low- $\Delta'^{17}O$ values.

5.4.1. *One-stage water-rock interaction*

Equilibrium fractionation curves such as those presented in Fig. 4 account for compositions resulting from the complete equilibration between water and rock, assuming water/rock ratio approaching infinity. However, the amount of seawater infiltrating into the erupted basalt is likely to be restricted due to the limited volume of fractures near the lava flow and connected porosity of the volcanic rocks. In this case, the

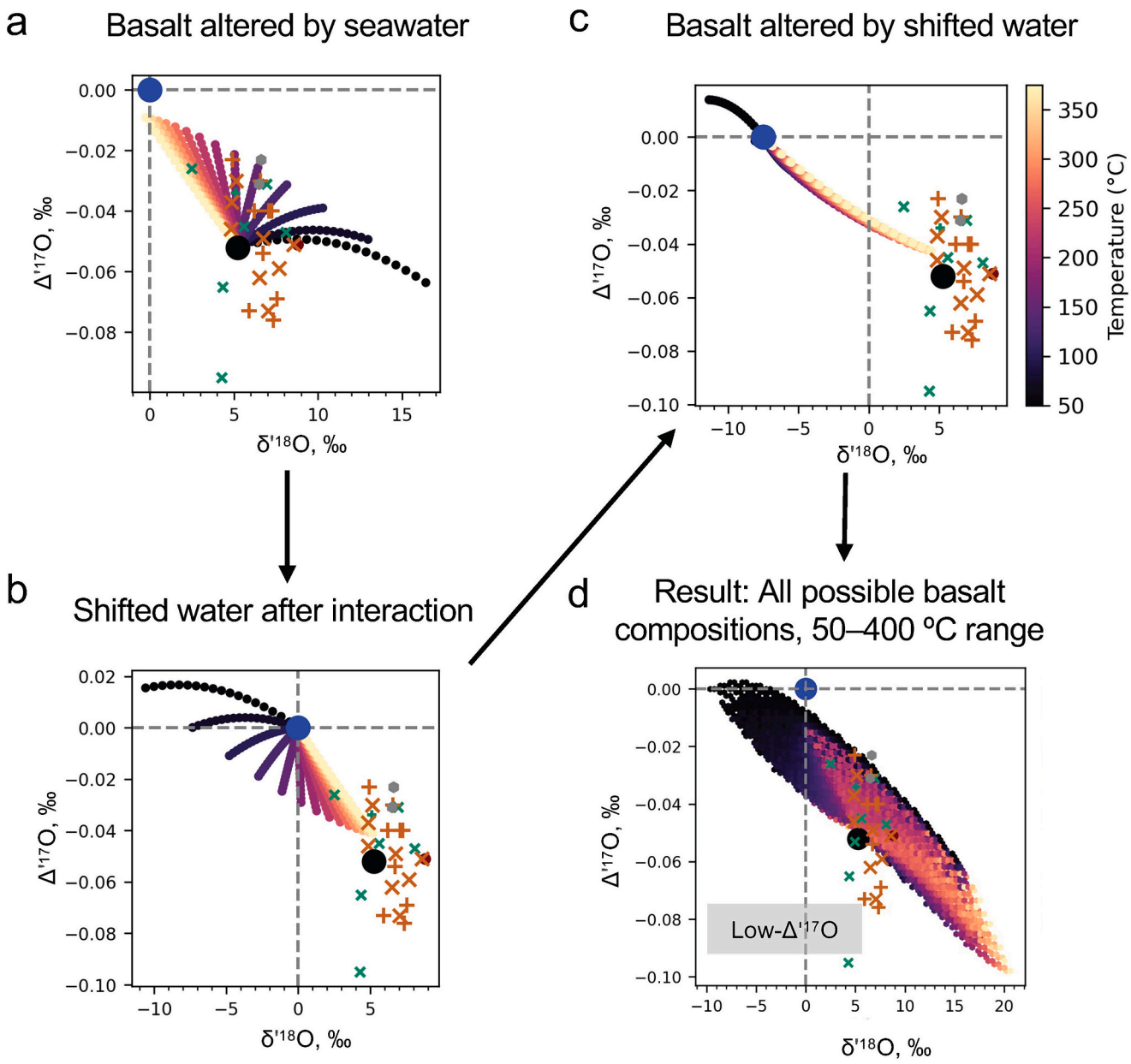

Fig. 7. Two-stage modelling of potential effects of water-rock interaction on triple oxygen isotopic rock compositions resulting from interaction with modern seawater. Different water/rock ratios (0.1 to 1) are shown by dots along a path at each colour-coded temperature. (a) The first phase interaction at a temperature range of 50–400 °C generates possible compositions of rocks that may result from this interaction. (b) Compositions of the shifted water after this interaction. (c) One of the water compositions derived in (b), namely $\delta'^{18}O = -7.5$ ‰, $\Delta'^{17}O = 0$ ‰, is used to interact with an unaltered basalt, showing the resulting rock compositions; (d) all possible outcomes of interaction between shifted waters in (b) with basalt. Colour coding in (d) reflects the temperature on the first (a, b, d) and second (c) phases. Note that the envisioned process of water-rock interaction explains all but low-$\Delta'^{17}O$ samples. Samples are plotted as in Fig. 5. Python code and instructions are available in Supplementary Materials.

resulting rock $\delta^{18}O$ and $\Delta'^{17}O$ compositions will be a combination of the equilibrium endmember and the initial basaltic rock composition. For low water/rock ratios, rather exotic $\delta^{18}O$ and $\Delta'^{17}O$ compositions of shifted waters are possible.

To assess these effects, we calculated the entire extent of possible whole-rock oxygen isotope compositions for a range of water/rock ratios (water fraction ranges from 0.1 to 1.0; water + rock = 1), with hydrothermal temperatures ranging from 50 to 400 °C. For these calculations, we use a simple mass-balance mixing model that is summarized by the following equation (after Wostbrock and Sharp, 2021):

$$\delta^x O_{rock\ final} = \frac{1000X + \alpha(X \bullet \delta^x O_{rock\ initial} - X \bullet \delta^x O_{water\ initial} - \delta^x O_{rock\ initial} - 1000X)}{\alpha X - \alpha - X} \quad (9)$$

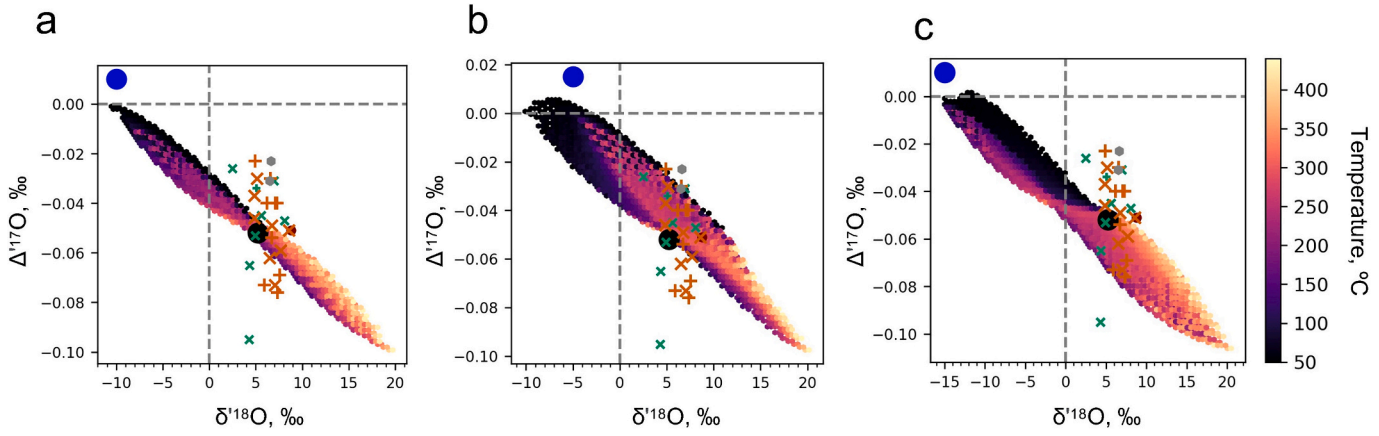

Fig. 8. Simulation of potential effects of water-rock interaction on triple oxygen isotopic rock compositions resulting from interaction with assumed Archean seawaters: a) Archean-I, $\delta'^{18}O = -10$ ‰, $\Delta'^{17}O = 0.01$ ‰, b) another assumption of the Archean-II, $\delta'^{18}O = -5$ ‰, $\Delta'^{17}O = 0.015$ ‰. Two-stage modelling is performed (details described in Fig. 7 caption and in text). Both figures cover all datapoints (withing $\Delta'^{17}O$ precision of ±0.01 ‰), except the lowest two most $\Delta'^{17}O$-depleted datapoints. Same symbols as Fig. 5. Python code and instructions are available in Supplementary Materials.

where X reflects water content (1 is water-dominated, 0 is rock-dominated system) and α is a fractionation factor.

Fig. 6a shows one-stage modelling for modern seawater and mantle, showing that the observed low-$\Delta'^{17}O$ compositions of the SHC rocks cannot be entirely explained by such interaction.

The results of interaction between typical basalts with mantle-like isotopic composition with more depleted Archean seawater ($\delta'^{18}O = -5$ ‰, $\Delta'^{17}O = 0.015$ ‰) are shown on Fig. 6b. These new parameters do not provide a better fit for the low-$\Delta'^{17}O$ samples. Even considering even more depleted Archean seawater ($\delta^{18}O = -10$ ‰, $\Delta'^{17}O = 0.01$ ‰), the low-$\Delta'^{17}O$ samples are not accounted for and this scenario would be inconsistent with the majority of the normal to high-$\Delta'^{17}O$ samples (Fig. 6c).

Fig. 6d represents the results of interaction between water with a $\delta'^{18}O$ and $\Delta'^{17}O$ range that corresponds evaporite waters (Surma et al., 2015), although there is no independent evidence for its existence during the formation and alteration of SHC basalts. However, a two-stage interaction involving underlying chemical sediments can provide a possible origin for such waters, without requiring evaporites. In summary, one-stage water-rock interaction can explain only half of the measured range of $\delta^{18}O$ and $\Delta'^{17}O$ values.

5.4.2. *Two-stage water-rock interaction producing large-scale $\Delta'^{17}O$ variations*

Seawater migration through fractures in seafloor rocks with water/rock ratios much less than infinity results in a shift of their composition (Gregory and Taylor, 1981). We used a two-stage model (Fig. 7; the Python code is available in Supplementary Material "2-stage modelling.py") to assess the possible triple oxygen isotopic compositions derived from such water/rock interaction:

1. The first stage of water-rock interaction generates a range of $\delta'^{18}O$ and $\Delta'^{17}O$ values in both the rocks and waters, and the composition of isotopically shifted water is calculated. This calculation is similar to that of the one-stage procedure, involving equilibrium fractionations and mixing, but in addition to the rock (Eq. 9, Fig. 7a), we calculate the shifted water composition (Fig. 7b) following:

$$\delta^x O_{water\ final} = \frac{1000 - 1000 \bullet \alpha + \delta^x O_{rock\ final}}{\alpha} \quad (10)$$

2. The second stage allows to calculate all possible rock compositions, using rock interaction with these shifted waters (instead of just pristine single composition seawater of assumed fixed isotopic value), looping through the same range of temperatures and water/rock ratios (Fig. 7c). Subsequently, we acquire the field of all possible rock compositions derived by such process by relying on the starting SMOW (0 ‰, 0 ‰ in $\delta'^{18}O$, $\Delta'^{17}O$ space) (Fig. 7d) as a reference. Geologically this can be visualized that pre-reacted (pre-exchanged, this isotopically shifted) Stage 1 waters are drawn to react with already reacted rocks, for example in a different rock layer.

This two-stage process results in a wider compositional field capable of explaining many low-$\Delta'^{17}O$ values plotting below the modern SMOW-basalt fractionation line, even with a modern seawater starting composition. Nonetheless, even after consideration of the error on $\Delta'^{17}O$ (±0.01 ‰), many datapoints remain difficult to explain by interaction with seawater characterized by modern-like compositions, even after being isotopically shifted by basalts (Fig. 7d). Archean seawater with lower $\delta'^{18}O$ of −10 ‰ or − 5 ‰ could, however, account for most of the SHC basalt compositions (Fig. 8).

We next used a Monte Carlo simulation based on our one- and two-stage models. First, we generated a random set of possible $\delta'^{18}O$ and $\Delta'^{17}O$ shifted water compositions ($\delta'^{18}O$ from −15 to +10 ‰, $\Delta'^{17}O$ from −0.05 to 0.03 ‰). Then, we calculated the full range of rock composition that might be result from interaction with such shifted waters, according to the algorithm described above. Simulation was run until the number of input parameter sets that successfully explain the observed rock compositions reached 200,000 (Fig. 9). We defined all rock modeled compositions with $\Delta'^{17}O > -0.06$ ‰ as low and those with $\Delta'^{17}O > -0.02$ ‰ as high. We also applied simulation to the rocks with the lowest $\Delta'^{17}O$ (< −0.075 ‰, Fig. 9e, f).

The Monte Carlo simulation shows that all high values can be reproduced by the modern SMOW both in one- and two-stage models (Fig. 9a, b), while lowermost values require interaction with water of $\delta'^{18}O < -10$ ‰ at $\Delta'^{17}O = 0.00$ ‰ and $\delta'^{18}O < -13$ ‰ at $\Delta'^{17}O = 0.01$ ‰ (Fig. 9c-f). Supplementary Fig. S3 presents the range of parameters (temperature and water fraction) that account for the samples with $\Delta'^{17}O$ values less than −0.06 ‰ through a two-stage interaction with seawater. The seawater characteristics include $\delta'^{18}O$ values from −7.8 ‰ to −7.6 ‰ and $\Delta'^{17}O$ values from −0.012 ‰ to 0.022 ‰. This figure demonstrates a wide range of permissible parameters with temperatures ranging from 323 to 673 K for the first stage and from 328 to 439 K for the second stage, as well as water fractions ranging from 0.11 to 1 in the first stage and from 0.57 to 1 in the second stage. The wide range of parameters ensures that at least some overlap with those plausible in natural systems. This result has several implications:

1) Our data and two-stage modelling generally favor the low-$\delta^{18}O$ values for Precambrian seawater (Kasting et al., 2006; Jaffrés et al., 2007).

2) Alteration of basalt by a water whose composition previously was

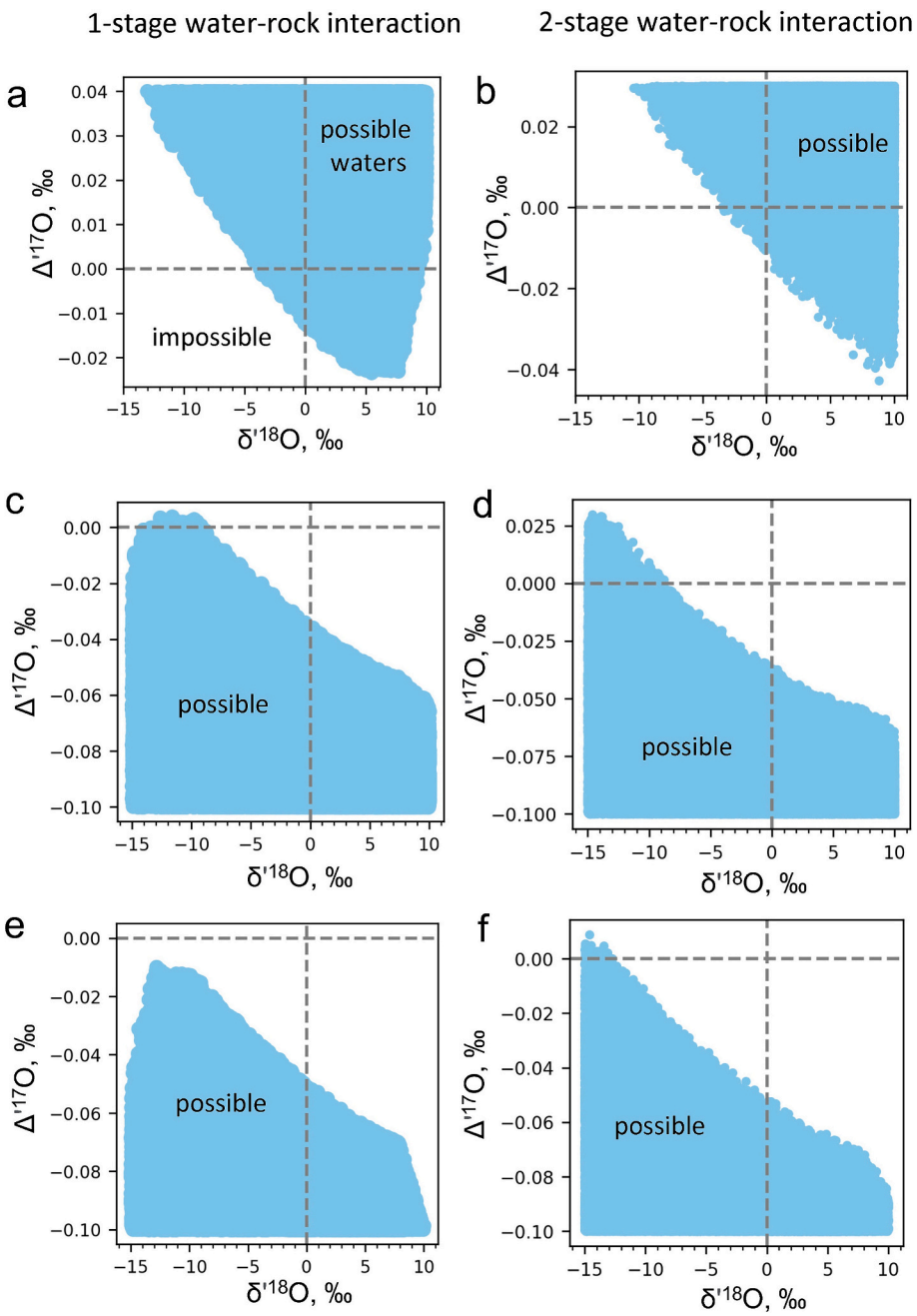

Fig. 9. The result of Monte Carlo simulations for 1- and 2-stage models of basalt-seawater interaction. The blue field corresponds to the water compositions capable of producing altered basalt with a certain composition: a, b – high $\Delta'^{17}O$ (> −0.02), c, d – moderately low $\Delta'^{17}O$ (<−0.06), and e, f – low $\Delta'^{17}O$ (<−0.075) at $\delta^{18}O$ between 4 and 6. Python code and instructions are available in Supplementary Materials. (For interpretation of the references to colour in this figure legend, the reader is referred to the web version of this article.)

shifted during interaction with a compositionally similar basalt has little effect on the overall $\delta^{18}O$ and $\Delta'^{17}O$ range of possible resulting rock compositions.

3) The most ^{17}O depleted and enriched rocks cannot be produced by interaction with a single and constant seawater composition. In other words, the fields of seawater composition in Fig. 9b and d (high and low $\Delta'^{17}O$ respectively) do not overlap. This implies that the waters that formed low- and high-$\Delta'^{17}O$ rocks had different compositions in $\Delta'^{17}O$, resulting from the described processes of shifting and mixing.

5.4.3. Interaction with overlying chemical sediments

Metasediments such as BIF and quartz-rich detrital sediments, are commonly found in association with the metavolcanic rocks in the SHC (e.g., Fig. 2a). Therefore, the low-$\Delta'^{17}O$ water that we infer as necessary in our models, may simply be explained by an isotopic shift caused by previous interaction with overlying sediments (carbonates or silica-rich chemical metasedimentary rocks; Fig. 2) (Wasilewski et al., 2019). To assess the possible effects of seawater interaction with sediments, we repeated the calculations described previously using hypothetical cherts (100 wt% SiO_2), carbonate (100 wt% $CaCO_3$) and actual Nulliak metasediments. The initial isotopic compositions corresponding to equilibrium with water at 30 °C were assigned as follows: $\delta'^{18}O = 36.4$ ‰ and $\Delta'^{17}O = -0.125$ ‰ for cherts, $\delta^{18}O = 27.7$ ‰ and $\Delta'^{17}O = -0.079$ ‰ for carbonate, and $\delta'^{18}O = 17.85$ ‰ and $\Delta'^{17}O = -0.078$ ‰ for metasedimentary rocks. Calculations using water that has previously reacted with cherts and carbonate are capable of producing both high- and low-$\Delta'^{17}O$

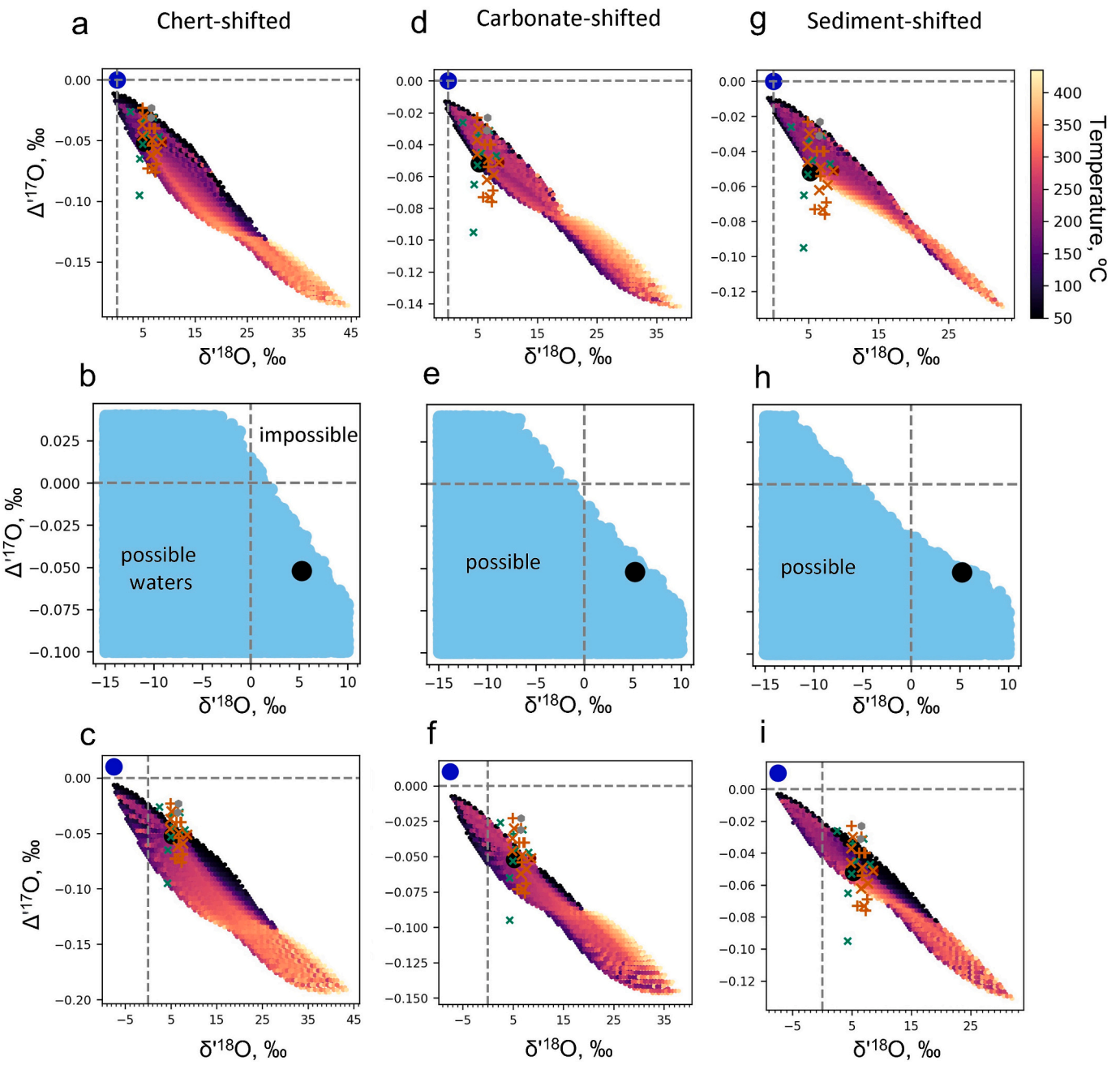

Fig. 10. The result of Monte Carlo simulations for 2-stage model of basalt—sediment-seawater interaction using typical sediments showing water compositions capable of explaining explain the observed low-$\Delta'^{17}O$ values (blue filed). First two simulations (a-d) were conducted for silica and carbonate endmembers, sediment-shifted simulation (e, f) with fractionation factors calculated for the actual sediments from the Saglek-Hebron Complex. (For interpretation of the references to colour in this figure legend, the reader is referred to the web version of this article.)

values from a very wide range of water composition, including modern seawater for cherts and slightly depleted seawater (−1 ‰) for carbonates (Fig. 10a-f). The SHC detrital sediments provided a more restricted field, with $\delta'^{18}O < -6$ ‰ being able to explain the whole range of observed compositions, including the lowest measured isotopic compositions (Fig. 10g-i).

5.5. Comparison with other >3.7 Ga altered basalts

The only other set of Eoarchean, and perhaps Hadean, volcanic rocks ever analyzed for triple oxygen is from the 4.3–3.8 Nuvvuagittuq greenstone belt in Canada (Bindeman and O'Neil, 2022). Unlike the rocks from the SHC, the Nuvvuagittuq rocks did not yield $\Delta'^{17}O$ values lower than those of the mantle (Fig. 4), hence, can be explained by our one-stage equilibrium fractionation and/or mixing model between modern seawater and basalt with mantle-like isotopic compositions (Fig. 6a). Our two-stage model Monte-Carlo simulation demonstrates that seawater with $\delta'^{18}O = -5$ ‰ can also adequately explain rocks with both mantle-like and elevated $\Delta'^{17}O$ values (Fig. 8a). Therefore, while the measurements reported in (Bindeman and O'Neil, 2022) do not necessarily require low-$\Delta'^{17}O$ Eoarchean seawaters, they also do not contradict their possible existence.

5.6. Implication for using hydrothermally-altered rocks as proxies into seawater $\delta^{18}O$ values

Our modelling resulting from the isotopic compositions of the SHC oceanic section is supportive of moderately depleted Eoarchean seawater with $\delta^{18}O \approx -7.5$ ‰ (−5 to −10 ‰). However, the detailed investigation of the oceanic crustal section of the SHC suggests that altered oceanic rocks also record a complex exchange history between overlying and intercalated chemical sediments and seawater entering the hydrothermal system affecting the basaltic rocks. More broadly, given the described mechanics of seawater-rock interaction enabled by considering triple O isotopes, the modelling indicates the critical importance of "shifted" waters in explaining compositions observed in the rock record at any age. Although our models do not consider any reactive-transport isotope exchange and only account for equilibrium exchange and water shifting and mixing, it reflects the isotope record of shallow oceanic rocks. Potentially these models would favor "weak" seawater-oceanic crust coupling constrained independently by 2D reaction transport modelling (Kanzaki, 2020; Kanzaki and Bindeman, 2022), and may have preference over models that consider full-coupling. (In this context, "weak" seawater-oceanic crust coupling refers to a limited exchange of oxygen isotopes between seawater and oceanic crust. Conversely, "strong" coupling indicates a near-complete exchange of oxygen isotopes). Interaction with seawater at mid-ocean ridges is assumed to account for 80 % or more of total oxygen 17 and 18 fluxes into the oceans (Wallmann, 2001), while Kanzaki and Bindeman (2022) model generates shifted waters via examining kinetics of water-rock interaction in 2D. Our study does not involve kinetics of oxygen isotope exchange of water-rock interaction but instead utilizes a combination of equilibrium fractionations of triple oxygen isotopes and fluid mixing.

If the role of water-rock interaction at mid-ocean ridges is indeed much less important than previously thought because of the early interaction of seawater with both chemical sediments and top layers of basaltic crust, then 1) the ability of ophiolite sequences to record the seawater isotopic composition is diminished, as we demonstrate by the associated water shifts that permit a wide range of input, and 2) isotopic impact provided by seawater-rock interaction is also reduced in estimating global ^{18}O and ^{17}O mass fluxed from the mantle to the hydrosphere. Furthermore, if the overall role of mid-ocean ridge–water interaction on O isotopes is significantly diminished, then weathering (the second most important flux into the ocean) becomes much more important in controlling the $\delta^{18}O$ value of the standing hydrosphere. Thus, low- $\delta^{18}O$ Archean oceans are possible without supposing substantially different extent of mid-ocean ridge–water interaction that would contradict rates of plate tectonics (Holland, 1984).

6. Conclusions

1. We found high and low-$\delta^{18}O$ (4.6 to 8.6 ‰) and $\Delta'^{17}O$ (−0.08 to −0.02 ‰) values in Eoarchean metabasalts from the Saglek-Hebron Complex.

2. Significant number of the Saglek-Hebron metabasalts yielded $\Delta'^{17}O$ values lower than those of the mantle that cannot be explained by direct (one-stage) interaction with seawater with modern-like compositions. A two-stage water-rock interaction model accounts for the low $\Delta'^{17}O$ compositions assuming ocean water with $\delta'^{18}O$ less then −8 ‰ at $\Delta'^{17}O \geq 0$ ‰. Such water compositions are similar to some compositions previously proposed for early Archean seawater.

3. The coexistence of both high- and low-$\Delta'^{17}O$ metabasalts in the Saglek-Hebron Complex can only be explained by additional interaction with spatially intercalated sedimentary rocks. Thus, our modelling suggests that hydrothermally altered sections of exposed oceanic crust record complex interaction upstream, including one- and two-stage water and rock compositional shifts in $\delta'^{18}O$ and $\Delta'^{17}O$, and interaction with exposed chemical sediment-derived waters on top of the oceanic crust.

4. Our modelling reveals the critical importance of two-stage "shifted" waters in explaining the submarine rock isotopic record and the role of overlying chemical sediments in explaining their $\delta'^{18}O$ and $\Delta'^{17}O$ systematics. Without proper modelling of water-rock interaction, involving isotopic shifts and mixing of such waters, exposed sections of altered oceanic crust present only remote evidence of the original seawater.

5. Due to these isotopic shifts and fluid mixing, we favor "weak" seawater-oceanic crust coupling in explaining isotopic record in submarine basalts across the geological history. This potentially diminishes the relative role of submarine hydrothermal alteration in favor of surface weathering in explaining global $\delta'^{18}O$ fluxes in and out of the oceans, permitting both low-$\delta'^{18}O$ Archean oceans and their wide oscillations throughout history.

CRediT authorship contribution statement

A. Kutyrev: Writing – original draft, Visualization, Software, Methodology, Investigation, Conceptualization. **I.N. Bindeman:** Writing – review & editing, Writing – original draft, Methodology, Investigation, Funding acquisition, Data curation, Conceptualization. **J. O'Neil:** Writing – review & editing, Visualization, Validation, Investigation. **H. Rizo:** Writing – review & editing, Visualization, Validation, Investigation.

Declaration of competing interest

The authors declare that they have no known competing financial interests or personal relationships that could have appeared to influence the work reported in this paper.

Data availability

The data are available in the supplementary materials. The code is also published in the open-access repository: https://doi.org/10.5281/zenodo.12795578.

Acknowledgements

INB and AK thank NSF grant EAR 1822977 and Jim Palandri for analytical help. AK worked at the University of Oregon as a Fulbright Visiting Scholar. We thank the Nunatsiavut Government and Parks Canada for permission to work and sample in the Saglek-Hebron area, as well as the staff from the Torngat Mountains Base Camp and Research Station for their assistance during fieldwork. Fieldwork was supported by the Northern Supplement Research Discovery Grant program of the Natural Sciences and Engineering Research Council of Canada. Grants to JO (RGPIN 435589-2013) and HR (RGPIN-2015-03982 and RGPIN-477144-2015). This is Cardiff EARTH CRediT Contribution 24.

Appendix A. Supplementary data

Supplementary data to this article can be found online at https://doi.org/10.1016/j.chemgeo.2024.122378.

References

Alt, J.C., Teagle, D.A.H., 2003. Hydrothermal alteration of upper oceanic crust formed at a fast-spreading ridge: mineral, chemical, and isotopic evidence from ODP Site 801. Chem. Geol. 201 (3–4), 191–211. https://doi.org/10.1016/s0009-2541(03)00201-8.

Baadsgaard, H., Collerson, K.D., Bridgewater, D., 1979. The Archean gneiss complex of northern Labrador. 1. Preliminary U–Th–Pb geochronology. Can. J. Earth Sci. 16 (4), 951–961. https://doi.org/10.1139/e79-081.

Bauer, A.B., et al., 2020. Hafnium isotopes in zircons document the gradual onset of mobile-lid tectonics. Geochemical Perspectives Letters 1-6. https://doi.org/10.7185/geochemlet.2015.

Bindeman, I., 2021. Triple oxygen isotopes in evolving continental crust, granites, and clastic sediments. Rev. Mineral. Geochem. 86, 241–290. https://doi.org/10.2138/rmg.2021.86.08.
Bindeman, I.N., O'Neil, J., 2022. Earth's earliest hydrosphere recorded by the oldest hydrothermally-altered oceanic crust: Triple oxygen and hydrogen isotopes in the 4.3-3.8 Ga Nuvvuagittuq belt, Canada. Earth Planet. Sci. Lett. 586 https://doi.org/10.1016/j.epsl.2022.117539.
Bindeman, I.N., Serebryakov, N.S., 2011. Geology, petrology and O and H isotope geochemistry of remarkably 18O depleted Paleoproterozoic rocks of the Belomorian Belt, Karelia, Russia, attributed to global glaciation 2.4Ga. Earth Planet. Sci. Lett. 306 (3–4), 163–174. https://doi.org/10.1016/j.epsl.2011.03.031.
Bindeman, I.N., Ionov, D.A., Tollan, P.M.E., Golovin, A.V., 2022. Oxygen isotope (delta (18)O, Delta'(17)O) insights into continental mantle evolution since the Archean. Nat. Commun. 13 (1), 3779. https://doi.org/10.1038/s41467-022-31586-9.
Bowers, T.S., Taylor, H.P., 2012. An integrated chemical and stable-isotope model of the origin of midocean ridge hot spring systems. J. Geophys. Res. Solid Earth 90 (B14), 12583–12606. https://doi.org/10.1029/JB090iB14p12583.
Bridgewater, D., Schiøtte, L., 1977. On the origin of early Archaean gneisses: a reply. Contrib. Mineral. Petrol. 62, 179–191.
Bridgewater, D., Collerson, K.D., Hurst, R.W., Jesseasu, C.W., 1975. Field characters of the early precambrian rocks from Saglek, Coast of Labrador. Geological Survey of Canada 75 (1), 287–296.
Chase, C.G., Perry, E.C., 1972. The oceans: growth and oxygen isotope evolution. Science 177 (4053), 992–994. https://doi.org/10.1126/science.177.4053.992.
Collerson, K.D., Campbell, L.M., Weaver, B.L., Palacz, Z.A., 1991. Evidence for extreme mantle fractionation in early Archaean ultramafic rocks from northern Labrador. Nature 349 (6306), 209–214. https://doi.org/10.1038/349209a0.
Dixon, J.E., et al., 2017. Light stable isotopic compositions of enriched mantle sources: resolving the dehydration paradox. Geochem. Geophys. Geosyst. 18 (11), 3801–3839. https://doi.org/10.1002/2016gc006743.
Dodd, M.S., et al., 2017. Evidence for early life in Earth's oldest hydrothermal vent precipitates. Nature 543 (7643), 60–64. https://doi.org/10.1038/nature21377.
Eiler, J.M., 2001. Oxygen isotope variations of basaltic lavas and upper mantle rocks. Rev. Mineral. Geochem. 43 (1), 319–364. https://doi.org/10.2138/gsrmg.43.1.319.
Galili, N., et al., 2019. The geologic history of seawater oxygen isotopes from marine iron oxides. Science 365 (6452), 469–473. https://doi.org/10.1126/science.aaw9247.
Gregory, R.T., Taylor, H.P.J., 1981. An oxygen isotope profile in a section of cretaceous oceanic crust, Samail Ophiolite, Oman: evidence for δ18O buffering of the oceans by deep (>5 km) seawater-hydrothermal circulation at mid-ocean ridges. J. Geophys. Res. 86 (B4), 2737–2755. https://doi.org/10.1029/JB086iB04p02737.
Grossman, E.L., Joachimski, M.M., 2022. Ocean temperatures through the Phanerozoic reassessed. Sci. Rep. 12 (1), 8938. https://doi.org/10.1038/s41598-022-11493-1.
Hayles, J., Gao, C., Cao, X., Liu, Y., Bao, H., 2018. Theoretical calibration of the triple oxygen isotope thermometer. Geochim. Cosmochim. Acta 235, 237–245. https://doi.org/10.1016/j.gca.2018.05.032.
Holland, H.D., 1984. The Chemical Evolution of the Atmosphere and Oceans, 2. Princeton University Press.
Isson, T., Rauzi, S., 2024. Oxygen isotope ensemble reveals Earth's seawater, temperature, and carbon cycle history. Science 383 (6683), 666–670. https://doi.org/10.1126/science.adg1366.
Jackson, E.D., Shaw, H.R., 1975. Stress fields in central portions of the Pacific Plate: Delineated in time by linear volcanic chains. Journal of Geophysical Research (1896–1977) 80 (14), 1861–1874. https://doi.org/10.1029/JB080i014p01861.
Jaffrés, J.B.D., Shields, G.A., Wallmann, K., 2007. The oxygen isotope evolution of seawater: a critical review of a long-standing controversy and an improved geological water cycle model for the past 3.4 billion years. Earth Sci. Rev. 83 (1–2), 83–122. https://doi.org/10.1016/j.earscirev.2007.04.002.
Johnson, B.W., Wing, B.A., 2020. Limited Archaean continental emergence reflected in an early Archaean 18O-enriched ocean. Nat. Geosci. 13 (3), 243–248. https://doi.org/10.1038/s41561-020-0538-9.
Kanzaki, Y., 2020. Interpretation of oxygen isotopes in Phanerozoic ophiolites and sedimentary rocks. Geochem. Geophys. Geosyst. 21 (6) https://doi.org/10.1029/2020gc009000.
Kanzaki, Y., Bindeman, I.N., 2022. A possibility of 18O-depleted oceans in the Precambrian inferred from triple oxygen isotope of shales and oceanic crust. Chem. Geol. 604 https://doi.org/10.1016/j.chemgeo.2022.120944.
Kasting, J.F., et al., 2006. Paleoclimates, ocean depth, and the oxygen isotopic composition of seawater. Earth Planet. Sci. Lett. 252 (1–2), 82–93. https://doi.org/10.1016/j.epsl.2006.09.029.
Knauth, L.P., Lowe, D.R., 2003. High Archean climatic temperature inferred from oxygen isotope geochemistry of cherts in the 3.5 Ga Swaziland Supergroup, South Africa. GSA Bull. 115 (5), 566–580. https://doi.org/10.1130/0016-7606(2003)115<0566:HACTIF>2.0.CO;2.
Komiya, T., et al., 2015. Geology of the Eoarchean, >3.95Ga, Nulliak supracrustal rocks in the Saglek Block, northern Labrador, Canada: the oldest geological evidence for plate tectonics. Tectonophysics 662, 40–66. https://doi.org/10.1016/j.tecto.2015.05.003.
Korenaga, J., 2021. Was there Land on the early Earth? Life (Basel) 11 (11). https://doi.org/10.3390/life11111142.
Kutyrev, A., Bindeman, I., O'Neil, J., Rizo, H., 2024. Code for 1- and 2-stage oxygen fractionation and metamorphic dehydration modeling from "Seawater-oceanic crust interaction constrained by triple oxygen and hydrogen isotopes in rocks from the Saglek-Hebron complex, NE Canada", zenodo.org. https://doi.org/10.5281/zenodo.12795578.
Lepot, K., 2020. Signatures of early microbial life from the Archean (4 to 2.5 Ga) eon. Earth Sci. Rev. 209 https://doi.org/10.1016/j.earscirev.2020.103296.
Liljestrand, F.L., et al., 2020. The triple oxygen isotope composition of Precambrian chert. Earth Planet. Sci. Lett. 537 https://doi.org/10.1016/j.epsl.2020.116167.
Luz, B., Barkan, E., 2010. Variations of 17O/16O and 18O/16O in meteoric waters. Geochim. Cosmochim. Acta 74 (22), 6276–6286. https://doi.org/10.1016/j.gca.2010.08.016.
Lyons, T.W., Reinhard, C.T., Planavsky, N.J., 2014. The rise of oxygen in Earth's early ocean and atmosphere. Nature 506 (7488), 307–315. https://doi.org/10.1038/nature13068.
McGunnigle, J.P., et al., 2022. Triple oxygen isotope evidence for a hot Archean Ocean. Geology 50 (9), 991–995. https://doi.org/10.1130/g50230.1.
Miller, M.F., Pack, A., 2021. Why measure 17O? Historical perspective, triple-isotope systematics and selected applications. Rev. Mineral. Geochem. 86 (1), 1–34. https://doi.org/10.2138/rmg.2021.86.01.
Miller, M.F., Pack, A., Bindeman, I.N., Greenwood, R.C., 2020. Standardizing the reporting of Δ'17O data from high precision oxygen triple-isotope ratio measurements of silicate rocks and minerals. Chem. Geol. 532 https://doi.org/10.1016/j.chemgeo.2019.119332.
Morino, P., Caro, G., Reisberg, L., Schumacher, A., 2017. Chemical stratification in the post-magma ocean Earth inferred from coupled ^{146,147}Sm–^{142,143}Nd systematics in ultramafic rocks of the Saglek block (3.25–3.9 Ga; northern Labrador, Canada). Earth Planet. Sci. Lett. 463, 136–150. https://doi.org/10.1016/j.epsl.2017.01.044.
Morino, P., Caro, G., Reisberg, L., 2018. Differentiation mechanisms of the early Hadean mantle: Insights from combined ^{176}Hf-^{142,143}Nd signatures of Archean rocks from the Saglek Block. Geochim. Cosmochim. Acta 240, 43–63. https://doi.org/10.1016/j.gca.2018.08.026.
Muehlenbachs, K., 1998. The oxygen isotopic composition of the oceans, sediments and the seafloor. Chem. Geol. 1998 (145), 263–273.
Muehlenbachs, K., Clayton, R.N., 1976. Oxygen isotope composition of the oceanic crust and its bearing on seawater. J. Geophys. Res. 81 (23), 4365–4369. https://doi.org/10.1029/JB081i023p04365.
Nutman, A.P., Fryer, B.J., Bridgwater, D., 1989. The early Archaean Nulliak (supracrustal) assemblage, northern Labrador. Can. J. Earth Sci. 26 (10), 2159–2168. https://doi.org/10.1139/e89-181.
Perry, E.C.J., 1967. The oxygen chemistry of ancient cherts. Earth Planet. Sci. Lett. 3, 62–66. https://doi.org/10.1016/0012-821X(67)90012-X.
Peters, S.T.M., et al., 2019. Triple oxygen isotope variations in magnetite from iron-oxide deposits, Central Iran, record magmatic fluid interaction with evaporite and carbonate host rocks. Geology 48 (3), 211–215. https://doi.org/10.1130/g46981.1.
Peters, S.T.M., et al., 2020. >2.7 Ga metamorphic peridotites from Southeast Greenland record the oxygen isotope composition of Archean seawater. Earth Planet. Sci. Lett. 544 https://doi.org/10.1016/j.epsl.2020.116331.
Pope, E.C., Bird, D.K., Rosing, M.T., 2012. Isotope composition and volume of Earth's early oceans. Proc. Natl. Acad. Sci. USA 109 (12), 4371–4376. https://doi.org/10.1073/pnas.1115705109.
Robert, F., Chaussidon, M., 2006. A palaeotemperature curve for the Precambrian oceans based on silicon isotopes in cherts. Nature 443 (7114), 969–972. https://doi.org/10.1038/nature05239.
Ryan, B., Martineau, Y., 2012. Revised and coloured edition of 1992 map showing the Geology of the Saglek Fiord – Hebron Fiord area, Labrador (NTS 14L/2,3,6,7). In: Scale: 1:100 000. Government of Newfoundland and Labrador, Department of Natural Resources, Geological Survey, Map.
Schauble, E.A., Young, E.D., 2021. Mass dependence of equilibrium oxygen isotope fractionation in carbonate, nitrate, oxide, perchlorate, phosphate, silicate, and sulfate minerals. Rev. Mineral. Geochem. 86 (1), 137–178. https://doi.org/10.2138/rmg.2021.86.04.
Schiøtte, L., Bridgwater, D., Collerson, K., Nutman, A., Ryan, A., 1986. Chemical and isotopic effects of late Archaean high-grade metamorphism and granite injection on early Archaean gneisses, Saglek-Hebron, northern Labrador. Geol. Soc. Lond. Spec. Publ. 24 (1), 261–273.
Schmidt, M.W., Poli, S., 1998. Experimentally based water budgets for dehydrating slabs and consequences for arc magma generation. Earth Planet. Sci. Lett. 163 (1–4), 361–379. https://doi.org/10.1016/S0012-821X(98)00142-3.
Sharp, Z.D., Wostbrock, J.A.G., 2021. Standardization for the triple oxygen isotope system: waters, silicates, carbonates, air, and sulfates. Rev. Mineral. Geochem. 86 (1), 179–196. https://doi.org/10.2138/rmg.2021.86.05.
Sharp, Z.D., et al., 2016. A calibration of the triple oxygen isotope fractionation in the SiO2–H2O system and applications to natural samples. Geochim. Cosmochim. Acta 186, 105–119. https://doi.org/10.1016/j.gca.2016.04.047.
Shimojo, M., et al., 2016. Occurrence and geochronology of the Eoarchean, ~3.9 Ga, Iqaluk Gneiss in the Saglek Block, northern Labrador, Canada: evidence for the oldest supracrustal rocks in the world. Precambrian Res. 278, 218–243. https://doi.org/10.1016/j.precamres.2016.03.018.
Stakes, D.S., O'Neil, J.R., 1982. Mineralogy and stable isotope geochemistry of hydrothermally altered oceanic rocks. Earth Planet. Sci. Lett. 57, 285–304.
Surma, J., Assonov, S., Bolourchi, M.J., Staubwasser, M., 2015. Triple oxygen isotope signatures in evaporated water bodies from the Sistan Oasis, Iran. Geophys. Res. Lett. 42 (20), 8456–8462. https://doi.org/10.1002/2015gl066475.
Surma, J., Assonov, S., Staubwasser, M., 2021. Triple oxygen isotope systematics in the hydrologic cycle. Rev. Mineral. Geochem. 86 (1), 401–428. https://doi.org/10.2138/rmg.2021.86.12.
Taylor Jr., H.P., 1971. Oxygen isotope evidence for large-scale interaction between meteoric ground waters and Tertiary granodiorite intrusions, Western Cascade Range, Oregon. Journal of Geophysical Research (1896–1977) 76 (32), 7855–7874. https://doi.org/10.1029/JB076i032p07855.
Valley, J.W., Kitchen, N., Kohn, M.J., Niendorf, C.R., Spicuzza, M.J., 1995. UWG-2, a garnet standard for oxygen isotope ratios: strategies for high precision and accuracy

with laser heating. Geochim. Cosmochim. Acta 59 (24), 5223–5231. https://doi.org/10.1016/0016-7037(95)00386-X.
Veizer, J., et al., 1999. $^{87Sr/86}$Sr, δ^{13}C and δ^{18}O evolution of Phanerozoic seawater. Chem. Geol. 161 (1), 59–88. https://doi.org/10.1016/S0009-2541(99)00081-9.
Vho, A., Lanari, P., Rubatto, D., 2019. An internally-consistent database for oxygen isotope fractionation between minerals. J. Petrol. 60 (11), 2101–2129. https://doi.org/10.1093/petrology/egaa001.
Wallmann, K., 2001. The geological water cycle and the evolution of marine δ18O values. Geochim. Cosmochim. Acta 65 (15), 2469–2485. https://doi.org/10.1016/S0016-7037(01)00603-2.
Wasilewski, B., O'Neil, J., Rizo, H., 2019. Geochemistry and petrogenesis of the early Archean mafic crust from the Saglek-Hebron complex (Northern Labrador). Precambrian Res. 328, 321–343. https://doi.org/10.1016/j.precamres.2019.04.001.
Wasilewski, B., O'Neil, J., Rizo, H., Paquette, J.-L., Gannoun, A.-M., 2021. Over one billion years of Archean crust evolution revealed by zircon U-Pb and Hf isotopes from the Saglek-Hebron complex. Precambrian Res. 359 https://doi.org/10.1016/j.precamres.2021.106092.
Whitehouse, M.J., Dunkley, D.J., Kusiak, M.A., Wilde, S.A., 2019. On the true antiquity of Eoarchean chemofossils – assessing the claim for Earth's oldest biogenic graphite in the Saglek Block of Labrador. Precambrian Res. 323, 70–81. https://doi.org/10.1016/j.precamres.2019.01.001.
Wostbrock, J.A.G., Sharp, Z.D., 2021. Triple oxygen isotopes in silica–water and carbonate–water systems. Rev. Mineral. Geochem. 86 (1), 367–400. https://doi.org/10.2138/rmg.2021.86.11.